# INSTRUMENTATION ARCHITECTURE AND REAL-TIME CONTROL OF MICROTURBINE

**Thatiana Virgínia Granja Cruz**
Departamento de Engenharia Mecânica, Universidade de Brasília
Campus Universitário Darcy Ribeiro, Brasília, DF, Brasil
tvgranja@hotmail.com

**Janaína Gomes de Merícia**
Departamento de Engenharia Mecânica, Universidade de Brasília
Campus Universitário Darcy Ribeiro, Brasília, DF, Brasil
jana.mericia@terra.com.br

**Carlos Gurgel Veras**
Departamento de Engenharia Mecânica, Universidade de Brasília
Campus Universitário Darcy Ribeiro, Brasília, DF, Brasil
gurgel@unb.br

**Geovany Araújo Borges**
Departamento de Engenharia Elétrica, Universidade de Brasília
Campus Universitário Darcy Ribeiro, Brasília, DF, Brasil
gaborges@ene.unb.br

***Abstract***. *This work presents the architecture for instrumentation and real-time computer control of a microturbine. The microturbine is comprised of a turbocharger, combustion chamber connected to the compressor outlet, a multi-fuel injection system and a lubricating system. The instrumentation apparatus of the microturbine is composed of a rotation sensor, pressure transducer, thermocouples and a fuel electro-injector. The microturbine dynamic model was defined and identified based on experimental data. The design of a PID controller was carried off-line with the identified model. Experimental evaluations demonstrated a satisfactory control design with an improved dynamic performance of the microturbine.*

***Keywords***: *microturbine, electronic instrumentation, data acquisition, PID control*

## 1. Introduction

In the current days a great number of technologies are being explored for distributed generation. These include solar cells, fuel cells, wind turbines, and small gas turbines. Gas turbines, or "microturbines", are a relatively new development, which in combination with the outcome of high-speed electric generators can be designed to produce power in the range of 30 to 100 kW. The units are very simple and small, can be quickly installed, and run at relatively low-cost. Maintenance efforts are greatly reduced as there is only one moving part. The level of production of microturbines has, recently, reached a commercial scale, with thousands of units running all over the world in a diversity of applications. In addition, pollution and noise emissions are very low and the system may burn a variety of fuels, or either, any fuel (gas or liquid) that can be injected into the combustion chamber. Microturbines represent a new generation of electricity production technology which will feature the power generation with environmental benefits for the near future.

Recently, some research is being carried on instrumentation and control of such units. In (Ariffin and Munro, 1997), due to approximate dynamic model identification, a robust $H^{\infty}$ control design is proposed for an aircraft gas-turbine. Nonlinear neural network control has been applied in (Cordeiro and Simões, 1999) for pollutant control in the microturbine.

In Brazil, the technologies related to microturbines are under investigation. The *Laboratorio de Energia e Ambiente* from Universidade de Brasília has been conducting studies in the combustion chamber in (Madela *et al.*, 1999) placed between the compressor and the turbine of an automotive turbocharger. Different combustion chambers have been tested with a broad range of fuels, illustrated in Fig.1 (Santos, 2002). This work presents the components of instrumentation and real-time computer control architecture that might be applied in microturbines.

The manuscript is organized as follows. Section 2 presents the electronic instrumentation modules implanted in the microturbine. System identification and PID control design are described in Sections 3 and 4, respectively. Experimental results are discussed in Section 5, which is followed by the conclusions.

Figure 1. Microturbine real system

## 2. Microturbine Instrumentation

### 2.1. Rotating Speed Measurement

For the purpose of rotating speed measurement, the sensor requirements are robustness, high temperatures proof, 10.000 to 100.000 rpm range and size. Concerning compressor size constraints, since air entrance has reduced dimensions, the sensor should be small such that air flow blocking is minimized. Thus, a variable reluctance sensor has been chosen for this purpose (Doebelin, 1990). The sensor structure is composed basically of four parts: coil, screw, support and female screw, as it can be observed in Fig. 2. The sensor magnetic reluctance depends on the positioning of the shaft. An analog circuit for reluctance measurement has been designed. Figure 3(a) shows its output signal for 5500 rpm. Since only the fundamental signal frequency of this signal is of interest, a histeresis comparator has been used. The digital signal output is TTL compatible, illustrated in Fig. 3(b).

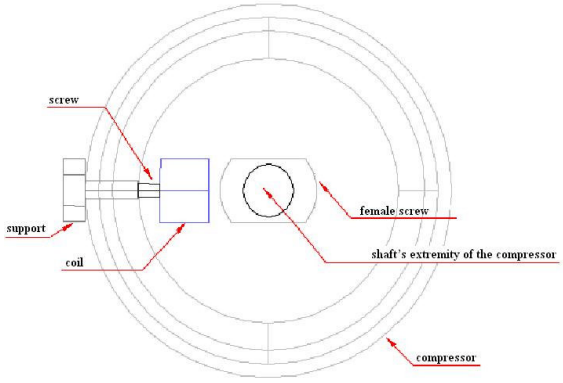


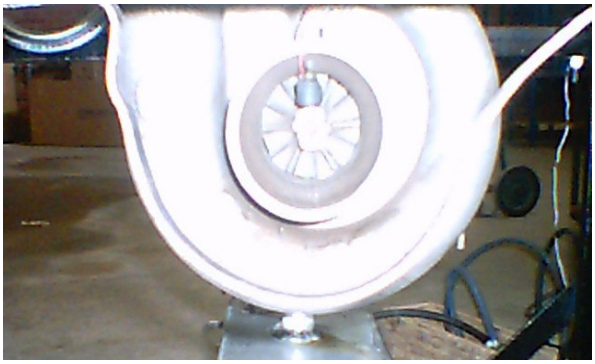

(a) Reluctance sensor schematic (b) Reluctance sensor real system

Figure 2. Schematic of the variable reluctance sensor

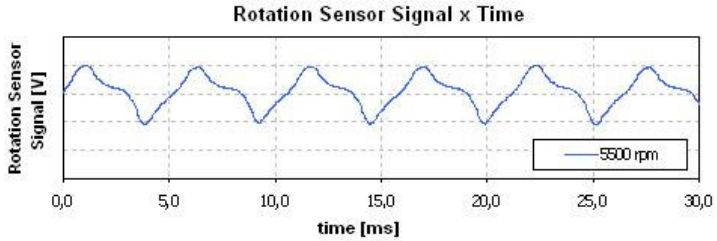


(a) Analog output

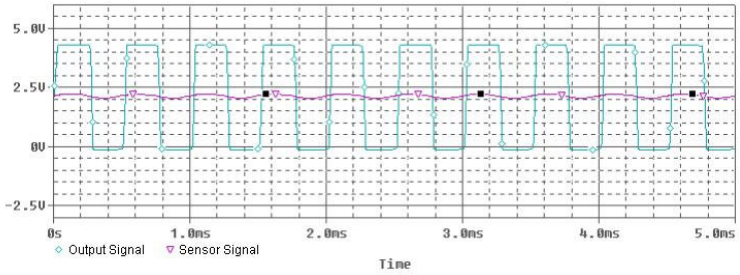


(b) Digital output vs analog signal

Figure 3. Rotating sensor analog and digital outputs for 5500 rpm.

### 2.2. Fuel Injection System

A bi-fuel injection system was designed and used to feed the microturbine. GLP gas was used as the main fuel for the system. This fuel guarantees the minimum condition for microturbine execution in idling mode. The gas injection was made through ¼ NPT connections with 5 bar pressure manually controlled.

The liquid fuel is the gasoline. A fuel electro-injector used in alcohol cars such GM Omega Suprema was adapted to control the fuel flow into the microturbine chamber. It was used in order to supply high fuel flow rates. Using this equipment it is possible to electronically control the fuel flow and change the operation states for the microturbine.

Turbine ignition is possible due to an automobile igniter was adapted with purpose of burning the fuel-air mixing inside the combustion chamber. This igniter was placed between the gas input connection and the gasoline electro-injector for strategic reasons described in the sequence. The GLP injector was placed in a 45º angle in a way the fuel flow path towards to the igniter to guarantees easy ignition. The GLP's angled path guarantees the gas recirculation and stable flame. Fig. 4 represents the microturbine's main elements placement diagram.

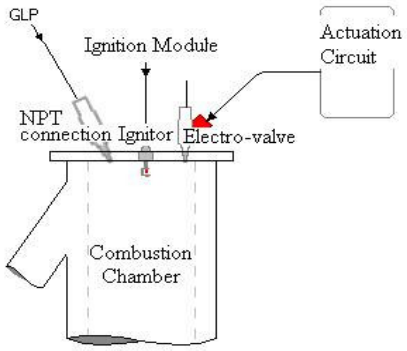


Figure 4. Schematic of fuel injection system.

The gasoline flow control is performed using the Pulse Width Modulation technique as input signal of power driven circuit of the gasoline electro-injector. An electronic circuit had been designed specially to charge the electrovalve following a digital electrical pulse. The electro-injector was calibrated using a calibrated burette in such way it was possible to obtain the relation between fuel flow and the electrovalve opening time and at the same time verify the frequency which the valve provides the higher fuel flow rate. In Fig. 5, it is observed fro the calibration curves that this device presents linear behavior sensor and higher flow rate for low frequencies.

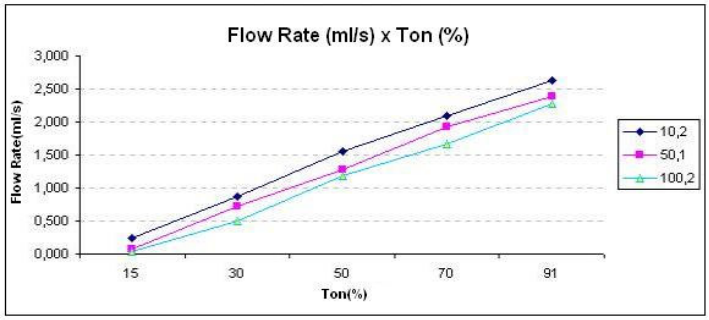


Figure 5. Electro-injector calibration curves.

### 2.3. Embedded Processing Unit

An 8-bit, 12MHz Intel 80C552 microcontroller-based board is responsible for data acquisition, control and actuator interfacing. The board contains RS-232 interface, 10-bit A/D converters, pulse width modulation (PWM) outputs, alphanumeric LCD, digital inputs, digital outputs, RAM and EPROM memories. Programming is done in C language in a IBM-PC computer, and downloaded to the board through serial interface (Schildt, 1996). Using this board, it was implemented an interrupt-driven solution for rotation speed measurement. Fuel injection is driven by a low frequency PWM signal (14 Hz).

## 3. Dynamic System Identification

Due nonlinear and distributed parameter characteristics of this system, mathematical modeling based on physical phenomena is extremely difficult. Therefore, experimental system identification techniques are used for determination of system dynamic behavior (Ljung, 1998). The identification signal choice reproduces the most common operation conditions. As the system could be affected by sudden transitions, step signal represents a good choice for test signal and persistently exciting to capture second order characteristics (e.g., oscillations). Identification experiment setup is depicted in Fig. 6.

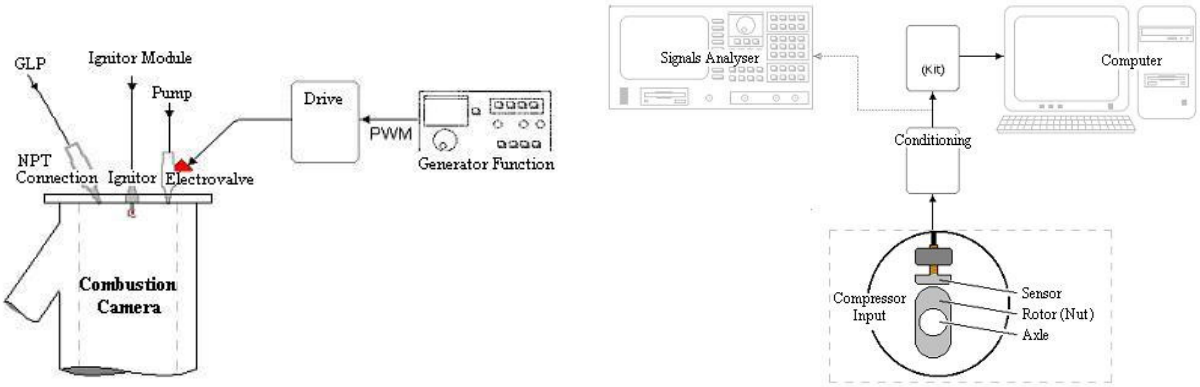


(a) Fuel injection setup (b) Speed measurement setup

Figure 6. Identification experiment setup

In this experiment, the microturbine was started up and it reached the idling state only depending on GLP resources. The gas outflow was adjusted until the microturbine rotation speed reaches its steady state in 60.000 rpm. The gas outflow was measured using a calibrated rotameter for GLP gas. The selected outflow was 90 l/min. When the rotation got stable in 60.000 rpm, the step signal was introduced in the system. Indeed, there were acquired data in response to two step signals, 0-50% and 0-70% duty cycle step variation at frequency of 14 Hz. The data acquisition started 5 seconds before the application of the step signal. The collecting time frame was 50 seconds and 500 points had been collected.

The data collected were time, microturbine output temperature, pressure in the beginning and end of the step signal and the corresponding fuel outflow for the duty cycle used. Seven experiments had been done. In five of them the step on duty cycle was 0-50% and for the others the cycles 0-70% of maximum value. Two graphs of the collected data are shown in the Fig. 7 and Tables 1-2. For the determination of the transfer function of the plant system, all of collected data had been considered.

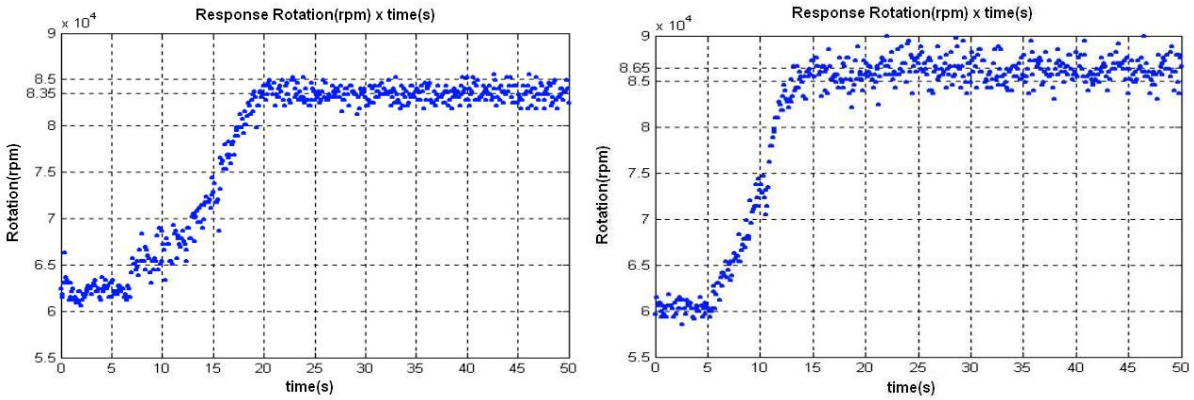


(a) 0-50% change of duty cycle (b) 0-70% change of duty cycle

Figure 7. Rotational speed dynamic response due to steps in injection system

Table 1. Flow, temperature and pressure for 50% duty cycle.

| Flow(ml/s) | Temperature(°C) | Pressure(Kgf/cm$^2$) |
|---|---|---|
| 0 | 530 | 1.07 |
| 0.95 | 556 | 1.20 |

Table 2. Flow, temperature and pressure for 50% duty cycle.

| Flow (ml/s) | Temperature (°C) | Pressure(kgf/cm$^2$) |
|---|---|---|
| 0 | 533 | 1.05 |
| 1.13 | 550 | 1.23 |

Simulink™ from Mathworks™ was used for the transfer function determination. Data analysis suggest the presented system is not a typical system of second order by the following reasons: the microturbine system response presented some non-linearities characteristics such as (transport) delay and derivatives around inflection points are very high, which is a characteristic of third or upper order systems.

For control purposes, the use of higher order models makes control design a more difficult task. Instead, using an approximate second order models is acceptable if the control design is robust against disturbances due to model error. Thus, it was decided that the transfer function could be replaced to a second order system with a delay and a zero, so the system will keep low losses of precision and high gain in simplicity characteristics.

According the curve, the dumped second order system approaches to with maximum small overshoot, and it was verified that the dumping coefficient would have to be next to 0.8. The dumped natural frequency was calculated from the criterion of 5% for the accommodation time (Ogata, 1998). The delay was determined from graphical analysis. A zero was placed in such a way that a faster transitory response is reached, reducing error model. The identified block diagram plant is presented in Fig. 8. Figure 9 superposes experimental and identified model curves of the microturbine plant.

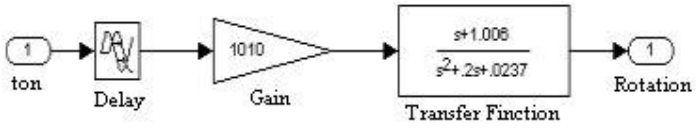


Figure 8. Block diagram of system plant.

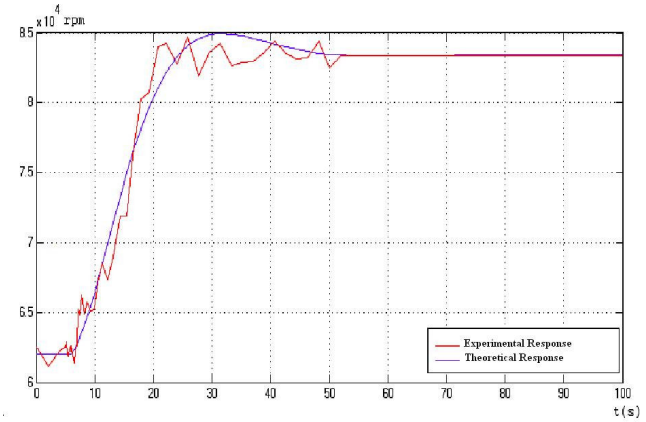


Figure 9. Experimental and identified system responses

## 4. PID Control Design

A PID controller was the first implemented control law of this system due to its clear advantages. In order to reduce the risk of adjusting the controller parameters in the real system, the design has been adjusted using the identified model following a well known practical design approach.

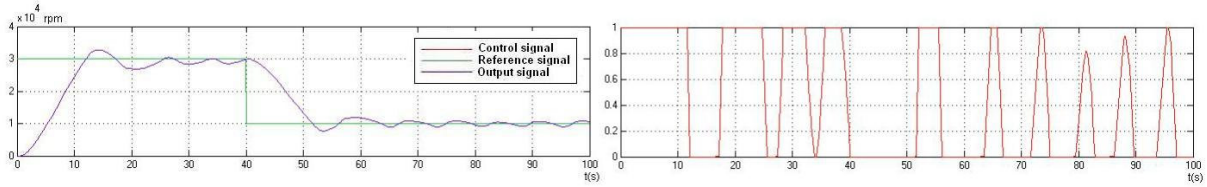


Figure 10. Proportional control response

The first step was the implementation of a proportional action, adjusting the gain so as to match the performance specifications. The results of these first tests are shown in Fig. 10. This figure shows a small stationary error and steady state oscillations. The overshoot is of about 6.7%. In terms of the control signal, the signal was working in limit cycle, which saturated the signal. This behavior is due to high proportional gain, but is undesirable because it may damage the actuator. On the other hand, smaller proportional gains may not result in fast system response.

In order to reduce the actuator oscillations, a derivative action had been adjusted. After adjusting the derivative gain, permanent regimen oscillations were reduced, but the stationary error remained, as illustrated in Fig.11.

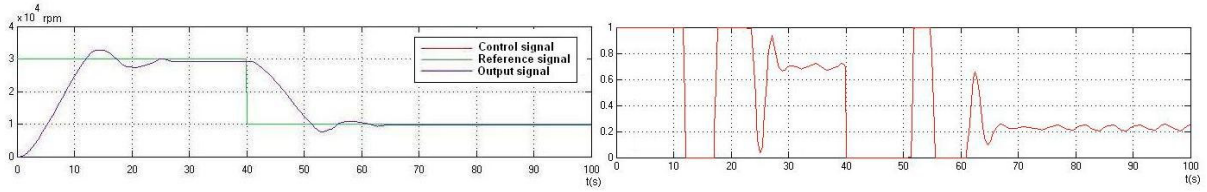


Figure 11. Derivative-proportional control response

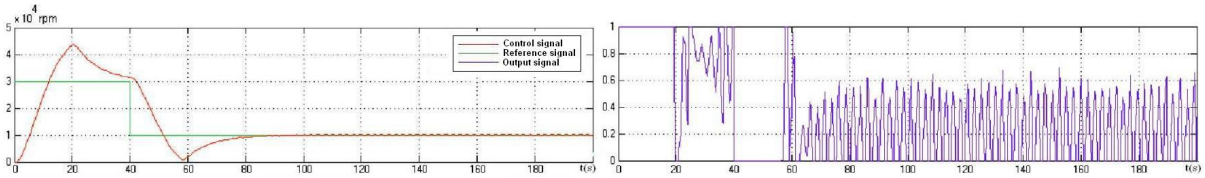


Figure 12. PID controller response

An integral control action was introduced by means of a small value of the integral gain in order to eliminate the stationary error and do not increase the instability risk. This control action was efficient, reducing the stationary error to zero, as illustrated in Fig. 12.

The existing oscillations in the control signal were eliminated by means of low-pass filters, as shown in Fig. 13. These filters were introduced in the output feedback path as well as in the input reference signal so that the system would not undergo sudden alterations. Figure 14 depicts the adjusted Simulink block model.

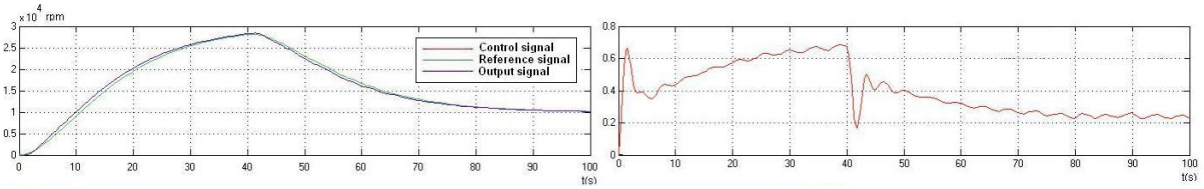


Figure 13. PID controller response with first-order low-pass filters

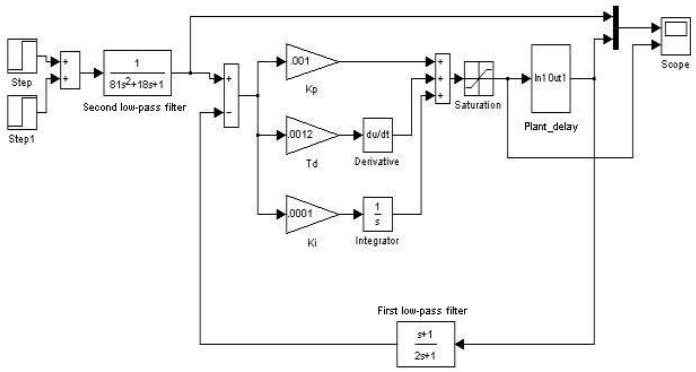


Figure 14. Complete system blocks diagram

## 5. Experimental Results

Before conducting experimental evaluations, the control system of Fig. 14 was evaluated for variable amplitude reference signals. The system response is shown in Fig. 15. It can be verified that the second order filter does undergo sudden alterations in the reference, allowing system ramp acceleration and preventing the inflection points of the actuator signal from entering the limit cycle. The feedback low-pass filter was designed to do not affect the system time constant.

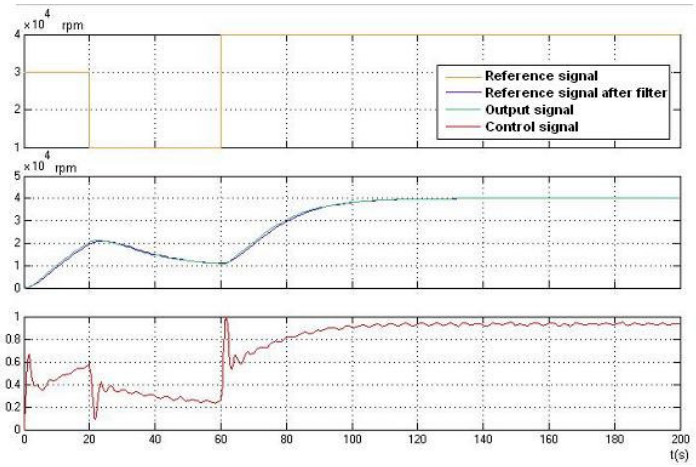


Figure 15. Control response of the identified model at different operating points

The simulated performance curves showed that the PID controller was satisfactory, with smooth response and no steady state error. Even such curves indicate system stability, a characteristic a root locus analysis was applied for verification of stability margins. The obtained stability margins confirmed this was a robust design.

For the experimental evaluation, a digital version of this controller has been implemented in the embedded microcontroller. The digital design used 100ms period, since the control system had a time constant of 20s. This period was approximately 200 times smaller than the system time constant. A well known rule of thumb for digital control

implementation says that the controller sampling period should be at about ten times smaller than the faster time constant of the system (Franklin et al., 1999). However, the high dynamics of the real system verified in the identification experiment justifies the use of a much smaller sampling period. On the other hand, a practical problem arises due to limited processing capabilities of the embedded processor. Indeed, due to the high processing time of the digital PID controller implementation in embedded processor, frequently interrupted by speed sensor signal, it was opted to implement on the proportional and integral actions. The obtained curves are shown in the Fig. 16. This final design presented satisfactory control performance.

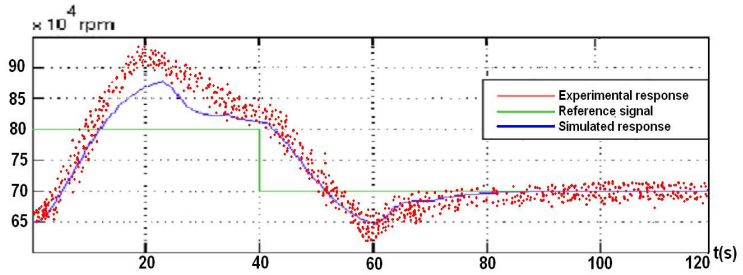


Figure 16. Real control PI implementation result. Identified system response is shown for comparison.

## 6. Conclusions

This paper described the instrumentation, system identification and control design of a GLP microturbine designed at the *Laboratorio de Energia e Ambiente* of *Universidade de Brasilia*. The electronic elements used in this work were entirely designed and mounted in the laboratory. Dynamic system identification resulted in a second-order delayed model relating actuator signal duty cycle to rotational speed mf the microturbine. A PID controller designed using the identified model presented satisfactory results in the real system, even without the derivative part.

## References


Ariffin, A. E., Munro, N., "Robust Control Analysis of a Gas-Turbine Aeroengine", IEEE Transactions on Control Systems Technology, Vol. 5(2), march, 1997.

Cordeiro, F. A., Simões, L.B., "Controlo de Poluentes numa Câmara de Combustão", Projeto de Graduação, Instituto Superior Técnico de Lisbo, Grupo Controle AUTOMAção Robótica (GCAR),1999.

Doebelin, Ernest O., "Measurements Systems", Mc Graw Hill Publishing Company, 1990.

Franklin, F. G., Powell, J. D., Workman, Michael, 1997, "Digital Control System", Addison Wesley , Third edition, 1999.

Lennart Ljung, "System Identification: Theory for the User", Prentice Hall, Second edition, 1998.

Madela, V., Silva, F., Carneiro, L. J, "Desenvolvimento da Câmara de Combustão de uma Microturbina, utilizando o código computacional PHOENICS", Projeto de Graduação, Universidade de Brasília, Departamento de Engenharia Mecânica, 1999.

Ogata, K., "Engenharia de Controle Moderno", Prentice-Hall do Brasil, 3ªedição, 1998.

Santos, A. F.,"Projeto e Estudo de uma Microturbina Multicombustível", Projeto de Graduação, Universidade de Brasília, Departamento de Engenharia Mecânica, 2002.

Schildt, H., "C Completo e Total", Makron Books , 3ª edição, 1996.


## 7. Responsibility notice

The author(s) is (are) the only responsible for the printed material included in this paper.